Report No. PC-NAS-004

FINAL REPORT

on

NASA Grant NSG-8002

INELASTIC SCATTERING

of

61 MeV PROTONS BY ^{207}Pb

July 1976

PAINE COLLEGE
1235 Fifteenth Street
Augusta, Georgia 30901

(NASA-CR-148531) INELASTIC SCATTERING OF 61 MeV PROTONS BY PB-207 Final Report, 1 Sep. 1975 - 31 Jul. 1976 (Paine Coll., Augusta, Ga.) 48 p HC $4.00 CSCL 20H

N76-28980

Unclas
G3/72 46760

Report No. PC-NAS-004

FINAL REPORT

on

NASA Grant NSG-8002

(September 1, 1975 through July 31, 1976)

INELASTIC SCATTERING

OF

61 MeV PROTONS BY ^{207}Pb

July 1976

Paine College
1235 Fifteenth Street
Augusta, Georgia 30901

Name of Institution: Paine College
1235 Fifteenth Street
Augusta, Ga. 30901

Title: Inelastic Scattering of 61 MeV Protons by ^{207}Pb

Principal Investigator: Dr. M. Owais
Assistant Professor of Physics, Division of Natural Science & Mathematics

Report Number: PC-NAS-004

TABLE OF CONTENTS

FOREWORD

The present report NO. PC-NAS-004 dated July 31, 1976 of Paine College, Augusta, Georgia, is the final report for NASA Grant NSG-8002 - This work was done in addition to the report NO. PC-NAS-003 entitled "Study of Single Crystals for Space Processing and the Effect of Zero Gravity". We would like to thank Mr. William J. McKinney, Grant Officer, National Aeronautics and Space Administration for his cooperation. We are also thankful to N.A.S.A. for the grant, without which this work would not have been completed.

ABSTRACT: Differential cross sections for the excitation of the first four neutron-hole states and the doublet at 2.61 MeV by 61.2 MeV protons have been measured. The data are analyzed in terms of both a purely collective model description and a microscopic model supplemented by macroscopic core polarization. A "realistic" two-body interaction is used and knock-on amplitudes are included. Core polarization is found to be important but represents a relatively smaller contribution than in most nuclei previously studied. A parallel analysis of similar data at lower proton bombarding energies reveals a surprisingly strong energy dependence of the reaction mechanisms.

1. INTRODUCTION

The differential cross sections have been measured for the excitation of the neutron-hole levels at 0.570 MeV, 0.898 MeV, 1.63 MeV, and 2.34 MeV and the doublet at 2.64 MeV using 61.2 MeV protons from the Oak Ridge Isochronous Cyclotron (ORIC).

Our earlier experiments showed that the more strongly structured cross sections for proton bombarding energy (E_p) of 61 MeV helped to stringently test microscopic models of inelastic scattering[1-5]). Both spin-flip and core polarization mechanisms were shown to be important for scattering from ^{89}Y at this energy[1,2]).

For both E_p=40 MeV and E_p=61 MeV, the excitation of the first 2^+, 4^+ and 5^- levels in ^{90}Zr was dominated by core polarization whose contribution is consistent with measured B(EL) values for these 2^+ and 5^- levels[2,6]). In our experiment on ^{90}Zr at 61 MeV, considerably less core polarization was required for the calculated cross sections for the 6^+ and 8^+ levels, and it appeared that either a more microscopic description of core polarization was needed or that non-central parts of the interaction should be used for the valence contributions[2]). Later calculations[7]) which included the spin-orbit part of the effective interaction for these proton excitations gave a better fit to the shapes of the measured cross sections.

The L=3 shape of the differential cross section for excitation of the $\frac{13^+}{2}$ single proton state at 1.63 MeV in ^{209}Bi

by 61 MeV protons clearly showed the importance of core polarization in inelastic scattering[3]), because of the strong coupling of the $h_{9/2}$ proton to the 3^- excitation of the ^{208}Pb core which had been predicted earlier[8]).

Current microscopic models, with core polarization treated collectively or microscopically, are discussed in references 3, 4, and 9 and references cited therein. Giant multipole resonances have been shown to be important at lower proton energies[10]), particularly for lighter nuclei and especially for states excited directly by the weak parts of the force. These effects are not believed to be important for low-lying natural parity states in medium and large-A nuclei with proton energies much above 30 MeV[11]).

Excited states of nuclei in the mass region near doubly-magic ^{208}Pb have been studied extensively in recent years, both experimentally and theoretically, because many of these states are expected to have simple structures involving either single particles or single holes coupled to this very strongly excited core. Much of this work is listed in reference 12, including that on inelastic scattering of protons.

The ^{207}Pb ground state has (to lowest order) one neutron hole in the doubly-closed shell of ^{208}Pb, and the first four excited states are predominantly single neutron-hole excitations[13]). For inelastic scattering, the ground state spin value of ½ highly restricts the possible values of angular momentum transfer L, so there are only a few 'allowed' amplitudes compared to the very large number involved in the excitation of the single-proton

state in ^{209}Bi at 1.63 MeV[3]). Because of the large matrix elements of the 2.614 MeV core state of ^{208}Pb to this 1.63 MeV state in ^{209}Bi, it was also not possible to study the relative importance of the valence contributions because core excitation completely dominates this transition. An additional reason for studying these neutron-hole transitions in ^{207}Pb with protons was that it appeared unlikely the spin-orbit part of the proton-neutron interaction would be important, and this may make it possible to see the effects of the tensor part of the nucleon-nucleon interaction. A similar experiment with 20.2 MeV protons had been reported[14]), so it would also be possible to study the energy dependence of the reaction mechanisms. Another experiment with 35 MeV protons was reported later[15,16]).

The experimental procedures are discussed in chapter 2. The collective model analyses and the effects of different optical model parameter sets are discussed in section 3.1.1 for data from this experiment and from the experiments[14,15,16]) at the lower proton energies of 20.2 MeV and 35 MeV. Our microscopic model calculations, with collective core polarization, are discussed in section 3.2 for the data at E_p=20.2 MeV and 61.2 MeV and are compared with similar calculations[15]) for the experiment with 35 MeV protons.

2. THE EXPERIMENT

The 61.2 MeV proton beam was obtained from the Oak Ridge Isochronous Cyclotron (ORIC) and the scattered protons detected at the focal plane of the broad-range spectrograph[17]) in Ilford 5.2 cm × 25.4 cm nuclear-track plates, which had 50 μm thick G5 emulsions and extra plasticizer. A 0.18 cm thick aluminium absorber was placed in front of the emulsions to stop heavy particles with the same magnetic rigidity, and also reduce the energy of the elastically scattered protons by about 4 MeV because the protons approach the focal plane at an angle of 37.5 degrees to the emulsion. A thin sheet of mylar, 25.4 μm in thickness, was placed between the aluminium absorber and the emulsions to prevent pressure and scratching which when developed would obscure the relatively faint proton tracks. Freshly made 'Brussels amidol' developer, a stop bath with acetic acid, and sodium thiosulphate fixer solution were used[18]). The target, enriched to 92.4% of ^{207}Pb and rolled to 6.5 mg/cm^2 thickness, was self-supported and purchased from the Isotope Sales Division of the Oak Ridge National Laboratory. The overall resolution ranged from 40 KeV at small angles to about 55 KeV at 100 degrees.

The data were accumulated in two separate beam runs. The relative normalizations of all the data were determined by making short exposures at different times during each run at a number of selected angles to observe the protons elastically scattered from ^{207}Pb with the same solid angle, effective target thickness and Faraday cup calibration as in the inelastic

scattering exposures of each run. From these 'elastic calibrations', absolute values of the inelastic cross sections were determined by assuming the elastic cross sections for ^{207}Pb to be the same as those measured earlier for ^{208}Pb at the same energy[19]). Overall 94 plates were taken with the spectrograph acceptance angle (in the scattering plane) of 3.0°, 41 plates with this angle at 1.0°, and 17 plates at 0.5°. With this angle at 3.0° counting tracks in a strip 2 cm length at the focal plane corresponds to a solid angle of 0.230 msr. At angles near those at which proton peaks for elastic scattering from ^{12}C and ^{16}O contaminants overlapped inelastic ^{207}Pb peaks, the smaller acceptance angles of 1.0° and 0.5° were used and the focal plane position shifted to narrow these contaminant peaks and allow a better determination of the ^{207}Pb cross sections. This technique has been discussed previously[1]).

The measured differential cross sections for the excitation of the first few ^{207}Pb levels and the doublet at 2.64 MeV are shown in table 1. The errors shown include those due to counting statistics, an estimate of the error made in the background subtraction and an estimate of the scatter in the track counting.

3. ANALYSES OF THE EXPERIMENTAL RESULTS

3.1 Collective (Weak-Coupling) Model Analysis

Of the six states reported from the present experiment, only the unresolved doublet[20,21]) at 2.64 MeV excitation is well

described by the weak coupling model. Although the first few excited states are believed to result from largely single neutron-hole excitations, for completeness collective model calculations were made for all of the transitions to the first six excited states. The observed transitions are described entirely by the excitation of phonons in the ^{208}Pb core with the single neutron-hole $(3p^{-1}_{1/2})$ in the ground state coupling to these phonons to form a doublet of states. Both the real and imaginary parts of the optical potential were deformed in our calculations and Coulomb excitation was included for quadrupole and octupole transitions. Our definition of the deformation parameter β_L does not included statistical factors, and should equal that extracted for a $0 \rightarrow L$ transition in ^{208}Pb if the weak coupling model is strictly valid. Our values of β_L are obtained from the other common definition by multiplying by the statistical factor $[(2J_i+1)(2L+1)/(2J_f+1)]^{\frac{1}{2}}$.

3.1.1 BEST FIT AND ENERGY DEPENDENT OPTICAL PARAMETERS

Because of previous discussions of ambiguities in normalization of collective model calculations (for example in references 16 and 22), we made two sets of collective model calculations for the measured cross sections at E_p=20.2 and 35 MeV (references 14, 15) and 61.2 MeV in the present experiment. The first set of calculations were made with 'best fit' optical model parameters, the 'first set' of reference 14 for E_p=20.2 MeV, those from reference 23 for E_p=35 MeV, and those from reference 19 for

E_p=61.2 MeV. The values of β_L we obtained using these 'best fit' parameters are listed as BFOM in column 5 of table 2 from an overall fit to the measured cross sections at all angles, not to the first prominent maxima in the angular distributions. In column 6 of table 2 $\beta_E-\beta_{61}$ is the percentage difference of the value of β_L we deduced at each lower energy from the value at 61 MeV.

The values of β_L shown in column 7 of table 2 were deduced from a second set of collective model calculations for E_p=20.2 MeV, 35 MeV, and 61.2 MeV, with the energy dependent parameters for ^{208}Pb of reference 24 which were derived from those of reference 25. The values of β_L in column 7 of table 2 labelled by HSOM (Halbert-Satchler optical model) were obtained from an overall fit to the measured cross sections at all angles, not to the first prominent maxima in the angular distributions. The percentage differences of these values of β_L from the values for 61 MeV are shown in column 8.

Column 9 of table 2 compares the value of β_L deduced at each proton energy with the HSOM parameters with the corresponding value of β_L in column 5 deduced at the same energy but with the BFOM parameters, expressing the differences as percentages.

For completeness, the values of β_L shown in column 10 for 35 MeV protons, labelled as BGOM, are those from reference 16 multiplied by the appropriate statistical factors $[(2J_i+1)(2i+1)/(2J_f+1)]^{\frac{1}{2}}$. The Bechetti and Greenlees optical model was used in that analysis. The last column of table 2

gives the percentage differences of these BGOM values of β_L from the BFOM values listed in column 5.

3.1.2 THE DOUBLET CENTERED AT 2.64 MeV

This doublet $(\frac{5^+}{2}, \frac{7^+}{2})$ at 2.64 MeV in ^{207}Pb is described as an octupole excitation of the core. The excitation energy of this doublet is in very good agreement[16,26]) with the energies of the underlying 3^- state in ^{208}Pb and the multiplet of states seen in ^{209}Bi. Figure 1 displays the excellent agreement between the 'best fit' collective model calculation with β_3=0.103. This value is almost identical with the final corrected 'best fit' values of β_3=0.101 and β_3=0.103 for the excitation by 61.2 MeV protons of the corresponding 3^- multiplet at 2.62 MeV in ^{209}Bi and the 3^- core at 2.615 MeV in ^{208}Pb, respectively[4]). All measured cross sections for ^{209}Bi in reference 3 should be increased by an experimental calibration factor of 1.060, which causes an increase of all values of β_L by a factor of 1.03. Although the shape of this BFOM calculation is an excellent fit to these data for multiplets in ^{207}Pb and ^{209}Bi and the 3^- state in ^{208}Pb, the collective model shape has small but definite differences from all three measured shapes. A direct comparison was made between these measured cross sections at 61.2 MeV by drawing a smooth curve through the data for the ^{207}Pb doublet at 2.64 MeV and comparing this 'data curve' with the measured cross sections for the corresponding excitations in ^{208}Pb and ^{209}Bi. All measured shapes are more alike than like the collective model shape. With a best value of β_3=0.103 for this ^{208}Pb cross

section[4]), this direct comparison yields β_3=0.100 ± 0.001 for the doublet in ^{207}Pb at 2.64 MeV and β_3=0.098 ± 0.001 for the multiplet in ^{209}Bi at 2.62 MeV.

The collective model calculation at 61.2 MeV, with Halbert and Satchler optical parameters for ^{208}Pb, yields values of β_3=0.100, 0.098, and 0.095 from direct comparison with the measured cross sections for these 'corresponding' excitations in ^{207}Pb, ^{208}Pb, and ^{209}Bi. The fall-off predicted by the HSOM collective model calculation is in poorer agreement with experiment than is the BFOM collective model calculation. This HSOM collective model calculation is shown for ^{207}Pb as the dashed curve in fig. 1.

3.1.3 THE STATES AT 0.570 MeV, 0.898 MeV, 1.63 MeV, and 2.34 MeV

Figure 2 shows a comparison between the collective model calculations and measured cross sections for the first few excited states in ^{207}Pb for E_p=61.2 MeV, with the 'best fit' parameters (BFOM) of reference 19 and the HSOM parameters of reference 24. The shapes of all these cross sections are well described by these collective model calculations, with the BFOM calculations providing a slightly superior description of the fall-off of $\sigma(\theta)$ with θ. Similar conclusions hold for analogous calculations at E_p=35 MeV with the exception that the angular distribution for the excitation of the 1.63 MeV state (L=7) is rather poorly described by the collective model.

Our BFOM collective model calculations are shown in fig. 4 for E_p=20.2 MeV. Both sets (BFOM and HSOM) of optical parameters give fairly good fits to the shapes of the data[14]), but the HSOM calculations are poorer for the L=7 transition.

There is a significant difference between the values of β_L in table 2 for these four transitions for E_p=20.2, 35, and 61.2 MeV. With the BFOM parameters, the values of β_L for E_p=20.2 MeV are larger than those for E_p=61.2 MeV by 7%, 24%, 59% and 56% for the L=2 (0.570 MeV), L=2 (0.898 MeV), L=4 (2.34 MeV), and L=7 (1.63 MeV) transitions, respectively. For E_p=35 MeV, the corresponding values of β_L are larger than those at 61.2 MeV by 22%, 14%, 14%, and 26% respectively. The value of β_2 from electromagnetic measurements for the L=2 transition to the 0.570 MeV state is the same as the value for E_p=61.2 MeV, but the electromagnetic value for the L=2 transition to the 0.898 MeV state is 14% smaller than the value for E_p=61.2 MeV[27]).

With HSOM parameters the trends are essentially the same, the values of β_L at E_p=20.2 MeV and 35 MeV are all larger than for E_p=61.2 MeV. The electromagnetic values for β_2 for the transition to the first excited state at 0.570 MeV is close to the HSOM value, but the HSOM value is larger than the electromagnetic value for the L=2 transition to the 0.898 MeV state.

Column 9 of table 2 reveals that the differences in the values of β_L with BFOM and HSOM parameters at the same proton energy are quite small, especially for the L=2 transitions to the first two excited states.

For either optical model parameter set, the energy dependence of β_2 for the first two transitions is relatively small and irregular but there is a smooth and strong decrease in β_L for the L=4 and L=7 transitions as E_p increases from 20 MeV to 61 MeV. Such an energy dependence of collective values of β_L is not without parallel. Previous (p,p') data for ^{89}Y showed a decrease in β_L for excitation of the low-lying states as the proton energy increased from 25 to 61 MeV[1]. The ground state of ^{89}Y has a $2p_{\frac{1}{2}}$ proton-hole ground state configuration and a low-lying spectrum roughly similar to ^{207}Pb. For ^{89}Y, β_2 decreases by 12% for the excitation of the $\frac{5}{2}^-$ proton-hole state compared to a decrease of 7% for the excitation of the $\frac{5}{2}^-$ neutron-hole state in ^{207}Pb for a similar increase in bombarding energy. The β_2 for the excitation of the $\frac{3}{2}^-$ proton-hole state in ^{89}Y decreases by 20% compared to a decrease of 19% for the excitation of the $\frac{3}{2}^-$ neutron-hole state in ^{207}Pb. The value of β_5 for the excitation of the $\frac{9}{2}^+$ state in ^{89}Y decreased by 25% compared to a decrease of 19% in β_4 and β_7 for these excitations in ^{207}Pb at 2.34 MeV and 1.63 MeV.

The electromagnetic values[27]) of β_2 are deduced from the weak-coupling model by assuming r_c=1.2 fm and $B(E2\uparrow)/e^2$ = 71 fm^4 and 61 fm^4 for the first and second excited states of ^{207}Pb respectively Although these β_2 are in close agreement with the values of β_2 for E_p=61.2 MeV, there is sufficient uncertainty in r_c to render the comparison somewhat inconclusive. Moreover, only protons contribute to γ-decay and the neutron and proton deformations may be different.

3.2. SHELL MODEL ANALYSIS INCLUDING CORE POLARIZATION

In the shell model description of inelastic scattering used here (semi-microscopic), the zero-order ground state of ^{207}Pb is taken to be a single $3p_{\frac{1}{2}}$ neutron hole in ^{208}Pb. The first four excited states are then reached by filling this vacancy from lower-lying neutron-particle states (single-hole excitations). This approximate description is consistent with single-nucleon transfer data[13]) which indicate that the levels at 0.570, 0.898, 1.63, and 2.34 MeV in ^{207}Pb correspond to the $2f_{5/2}$, $3p_{3/2}$, $1i_{13/2}$, and $2f_{7/2}$ neutron-hole states. To next order the neutron hole interacts with the ^{208}Pb core and polarizes it by inducing both neutron and proton particle-hole states. It has been shown in ref. 15 that the inclusion of these 1p-2h admixtures in a completely microscopic calculation enhances the cross sections predicted by the single-hole model by roughly a factor of 4, in reasonable agreement with the data for each of the first four excited states at E_p=35 MeV.

In this paper, those components of the wave function outside the single-hole space are represented by the collective model which has proven quite successful in describing the cross sections for the low-lying states of the core system. Consequently, the transition amplitude is composed of a valence and a core polarization part. The valence part is that associated with excitations within the zero-order shell model (single-hole excitations) and the core polarization term arises from the participation of the core. The strength of the core participation ($A_L=y_L\langle k\rangle$) as

defined in reference[2]) can in principle be deduced by knowing the effective charge (e_{eff}) for the corresponding transition[28]). However, since only the quadrupole effective charges are known for the transitions considered, A_L is treated as an adjustable parameter to be compared with those A_L which are deduced from other experiments. If the core excitations are isoscalar, A_L is related to the effective charge as described in ref. 2.

The formalism for calculating the valence[29,30]) and core[28]) contributions to inelastic scattering have been given elsewhere so that only the details peculiar to the calculations made here are given. Since the valence amplitudes arise from protons scattering from neutrons, the L-S force, which is strongest[31]) between like nucleons, was not included. The central part of the interaction is given by:

$$V_c(1,2) = -V\, e^{-0.37 r_{12}^2}$$

where V_{SE}=30.8 MeV and V_{TE}=41.8 MeV. This interaction has roughly the same small momentum components as the truncated Hamada Johnston interaction used in ref.[29]). For protons scattering from neutrons, this potential is more than an order of magnitude stronger for a spin-transfer (S) of zero than for S=1. Where indicated a tensor force given by:

$$V_T\,(1,2) = -V\, g(r_{12})\; S_{12}\; \underset{\sim}{\tau}_1 \cdot \underset{\sim}{\tau}_2$$

was included where S_{12} is given in ref. 30, g(r) is the regularized OPEP form given by equations (23 and 39) of ref. 30 and V=-3.94 MeV.

It is well known[32]) that magnetic moments and magnetic transitions are quenched relative to their single particle values when the effects of core polarization are included. This fact, together with the weak S=1 part of the central p-n interaction suggests that the S=1 amplitudes arising from the central part of the force be neglected and this is done throughout. Although these amplitudes interfere with those arising from the much stronger tensor force, the latter are also found to be relatively less important than might be expected, and the net effect of including the S=1 central force terms is negligible.

Recent evidence[33]) has suggested that it is important to include an imaginary term in the interaction inducing the transition. Since how to do this is poorly understood, the entire imaginary coupling (valence and core) was taken from the collective model prescription discussed in sect. 3.1 and normalized by the appropriate β_L. Since previous calculations have proven[15]) rather insensitive to the details of the radial wave functions, all orbitals in the present calculation were calculated assuming a binding energy of 7 MeV in a Woods-Saxon well having r_o=1.2 fm, a=0.7 fm and a spin-orbit force 25 times the Thomas term.

The BFOM parameters of reference 19 were used in all of the microscopic model calculations discussed below for the proton

energy E_p=61.2 MeV. To study the energy dependence of the excitation mechanism, similar calculations were made for the corresponding data at E_p=20.2 MeV, using the first set of optical parameters of ref. 14. Results of similar calculations at E_p=35 MeV were obtained from ref. 15.

3.2.1 THE 0.570 MeV STATE ($J^\pi = \frac{5}{2}^-$)

The valence amplitude for this transition arises from the excitation of a hole from the $3p_{1/2}$ level to the $2f_{5/2}$ level. This transition is dominated by LSJ=202. Figure 3a shows a comparison between the experimental and theoretical cross sections for E_p=61.2 MeV. The shape of the valence term (V) alone is seen to be in poorer agreement with the data than is the core (C) term alone. Despite the comparable contributions from the V and C terms (A_2=0.020), the complete cross section is in good agreement with the data. An analogous comparison for the excitation of this level at E_p=20.2 MeV is shown in fig. 4a. At this lower energy A_2=0.033. Although the valence term alone makes a relatively smaller contribution at the lower energy, the fit to the data is considerably worse.

Table 3 shows a comparison of the effective neutron charges e_{eff} deduced from the (p,p') experiments at 20.2, 35 and 61.2 MeV along with that deduced from the experimental B(E2). The effective charge obtained from the 61 MeV data for this transition is much smaller than that from the other experimental data.

One measure of the strength of the two-body interaction and its dependence on energy is given by the strength and energy variation of the volume integral (per nucleon) of the real part

of the empirical optical potential[25]). We show in parentheses in table 3 the values of A_L and e_{eff} which are extracted when we scale the volume integral of the two-body interaction (including exchange[34]) to match that of the empirical optical potential at each proton bombarding energy. These numbers are approximate since the calculations were not actually repeated. Instead use was made of the fact that the core and valence amplitudes (excluding the imaginary coupling) are almost completely in phase. For E_p=35 MeV the values of A_L and e_{eff} shown in parentheses are results of microscopic core polarization calculations from ref. 15.

3.2.2 THE 0.898 MeV STATE ($J^\pi = \frac{3}{2}^-$)

This transition corresponds to the excitation of a neutron hole from the $3p_{1/2}$ to the $3p_{3/2}$ level. This transition is mediated predominantly by LSJ=202. Figure 3b shows a comparison between the experimental and theoretical cross sections at E_p=61.2 MeV. A similar comparison is shown for E_p=20.2 MeV in fig. 4b. At E_p=61.2 MeV the valence term alone is in poor agreement with the data. When supplemented by the core polarization term (A_2=0.020), satisfactory agreement with experiment is obtained. At E_p=20.2 MeV (fig. 4b) the valence plus core (A_2=0.030) terms yield a much less satisfactorily-shaped cross section, particularly around θ_{cm}=80°. This relatively poor description of the cross section can be traced to the form-factor for this transition. In particular, the valence form-factor peaks well inside the nuclear surface and looks completely unlike the collective model form-factor known to describe the

shape of this cross section quite well. At both of these energies the V term is larger than the C term, V being relatively more important at 61 MeV than at 20 MeV. Like the $\frac{5}{2}^-$ state, the effective charge of 0.55 extracted from the 61 MeV data is much less than that obtained from the other experiments at 20 MeV and 35 MeV.

When the central valence interaction is normalized to the empirical optical model volume integral [25], at 61.2 MeV A_2=0.027 and e_{eff}=0.74.

3.2.3 THE 1.63 MeV STATE ($J^\pi = \frac{13}{2}^+$)

The excitation of this level proceeds primarily by the excitation of a neutron hole from the $3p_{1/2}$ to the $1i_{13/2}$ state. The LSJ=707 transfer dominates this transition. Figures 3c and 4c show a comparison between the experimental and theoretical cross sections at E_p=61.2 and 20.2 MeV respectively. At E_p=61.2 MeV the V and C terms together (A_7=0.010) provide an acceptable description of the angular distribution but one which is inferior to that predicted by the collective model alone. At E_p=20.2 MeV and with A_7=0.030 the fit to the experimental data is good. This results because of the very small contribution (<10%) that the valence term alone makes at the lower energy. The value of the effective charge deduced from the data at 61.2 MeV is found to be 0.23 which is a factor of 2 smaller than the value calculated in ref. 15, and is even smaller when compared to the value deduced from the (p,p') data at E_p=20.2 MeV.

When the central valence interaction is normalized to the volume integral of the optical potential from elastic scattering[25] at 61.2 MeV, A_7=0.012 and e_{eff}=0.28.

3.2.4 THE 2.34 MeV STATE ($J^\pi = \frac{7}{2}^-$)

The valence part of this transition corresponds to the excitation of a $3p_{1/2}$ neutron hole to the $2f_{7/2}$ level. For S=0, (and $(-)^L = \Delta\pi$) an (LSJ) transfer of (404) is required for this transition. Figures 3d and 4d show a comparison between the experimental and theoretical cross sections at E_p=61.2 and 20.2 MeV respectively. At 61 MeV the combined V and C amplitudes provide a reasonable description of the experimental cross section when A_4=0.015. The V plus C fit to the data is, however, slightly poorer than the collective model fit alone. At 20 MeV, a similar result obtains with A_4=0.038 except that the microscopic (V+C+I) fit to the data is considerably poorer than the macroscopic prediction alone. This occurs despite the relatively smaller contribution of the valence term at the lower energy. The effective charge deduced at 61 MeV is substantially smaller than those e_{eff} found from (p,p') data at E_p=20 and 35 MeV as well as that calculated in ref. 15 (see table 3).

When the central valence interaction is normalized to the empirical optical potential at 61.2 MeV, A_4=0.019 and e_{eff}=0.49.

3.2.5 TENSOR FORCE CONTRIBUTIONS

The tensor force only gives rise to S=1 amplitudes[30]. Since these are nearly incoherent with the S=0 amplitudes,

the contributions (direct and exchange) from the tensor force have been calculated separately. It has been shown[15] that the S=1 cross sections are overestimated for this nucleus by roughly a factor of three for the transitions considered here when only a single hole transition is considered. Consequently, the S=1 valence cross sections were divided by 3 before they were added to the S=0 terms. This roughly accounts for core polarization of the S=1 type. When included in this way the S=1 terms make very little difference (no change in A_L) in the full (S=0+S=1) cross sections for any of the transitions considered at E_p=61 MeV. Consequently, the S=1 terms were not calculated at E_p=20 MeV.

3.2.6 ENERGY DEPENDENCE

As can be seen in table 3, in order for these semi-microscopic model calculations to describe the experimental cross sections at both E_p=61 and 20 MeV, there must be a strong energy dependence of the core polarization strengths A_L (see column 6 of table 3). This energy dependence of A_L is much stronger than that for β_L when the collective model is used. This arises from the fact that the valence contributions to the cross sections fall off much slower with increasing energy than do the experimental cross sections. In fact, for the $\frac{13}{2}^+$ level, the valence contribution to the cross section <u>increases</u> by a factor of 2 in going from E_p=20 to E_p=61 MeV whereas the experimental cross section <u>decreases</u> by a factor of 0.64! Scaling the valence contributions to the empirical energy-dependent optical potential helps but does not resolve this

difficulty. Consequently, unless the other single particle amplitudes arising from a completely microscopic treatment of the core exhibit an energy dependence significantly different from that of the dominant single-hole amplitude, there appears to be a serious problem in regarding this transition as a simple one-step process (at least over this entire energy range). The above comment assumes that there is no large intrinsic energy dependence of V_{pn}. If, on the other hand, the extreme assumption is made that the A_L extracted at E_p=20 MeV are correct and energy independent then V_{pn} decreases dramatically with increasing energy becoming repulsive for the L=4 and L=7 transitions! This is in strong disagreement with the optical potential. If A_L decreases with increasing proton energy at the same rate as the β_L from the collective model, then V_{pn} must be considerably weaker than its "realistic" two-body value.

4. DISCUSSION

The presumably simple shell-model states excited in this experiment are found to be described in terms of the collective model with a significant energy dependence of the deformation parameters. Those β_2 deduced from experimental values of B(E2) are in best agreement with the β_2 found at 61 MeV.

The microscopic description of inelastic scattering (with macroscopic core polarization) provides a reasonable description of the shell-model states seen in this experiment. However, a consistent description of this experiment and a similar one at

E_p=20.2 MeV could only be achieved by allowing the core strengths (A_L) to decrease rapidly with increasing energy. Whether a completely microscopic description of this transition can describe completely the observed energy dependence within the framework of a one-step reaction mechanism is unknown since such a calculation has only been carried out at E_p=35 MeV. Such a calculation at the other proton bombarding energies could be very illuminating. For transitions as weak as these in ^{207}Pb the possibility of multiple excitation should be considered. Inclusion of such terms might help explain the increase in β_L (or A_L) as the bombarding energy is reduced.

It appears that whatever model is used to describe these transitions, it must effectively give rise to a surface peaked form-factor in order to describe the shape (and perhaps energy dependence) of the angular distributions. This may necessitate the use of a density dependent interaction. These conclusions are to be contrasted with those of Halbert and Sachler[24], who find an interaction similar to the one used here to be reasonably adequate (when exchange is included exactly) in explaining the excitation of ^{208}Pb over a similar range of energies when a completely microscopic description is used.

Because of the quenching of the S=1 contributions for these neutron-hole transitions, the effects of the tensor part of the nucleon-nucleon force were unfortunately negligible for these neutron-hole transitions. The core polarization contributions here were unusual as they were comparable with the valence contributions, so that the relative importance of these could be studied with more clarity than in experiments exciting

natural parity states in most other nuclei in which core polarization is generally much larger than the valence contributions.

ACKNOWLEDGEMENTS

The Principal Investigator gratefully acknowledges Dr. Alan Scott and Dr. W. G. Love for collaboration with this project; Dr. E. E. Gross and Dr. J. B. Ball for providing beam time from the Oak Ridge Isochronous Cyclotron; Mr. R. S. Lord, Mr. A. W. Riikola, Mr. M. B. Marshall and the cyclotron operation group for their friendly cooperation; Mr. A. F. Moore and Mr. Leon Garrett for assistance with track counting; and Mr. N. W. Herzen for assistance during some beam runs and with some of the data reduction.

REFERENCES

1. A. Scott, M. L. Whiten and W. G. Love, Nucl. Phys. A137 (1969) 445.

2. M. L. Whiten, A. Scott and G. R. Satchler, Nucl. Phys. A181 (1972) 417.

3. Alan Scott, M. Owais and F. Petrovich, Nucl. Phys. A226 (1974) 109.

4. Alan Scott, N. P. Mathur, F. Petrovich and G. R. Hammerstein, submitted to Nuclear Physics.

5. M. Owais, Alan Scott and W. G. Love, Bull Amer. Phys. Soc. 18 (1973) 721.

6. R. Hinrichs, D. Larson, B. M. Preedom, W. G. Love and F. Petrovich, Phys. Rev. C7 #5 (1973) 1981.

7. W. G. Love, Nucl. Phys. A192 (1972) 49.

8. B. R. Mottelson, J. Phys. Soc. Japan Suppl. 24 (1968) 96; I. Hamamoto, Nucl. Phys. A126 (1969) 545; N. Auerbach and N. Stein, Phys. Lett. 28B (1969) 628; R. Broglia, J. Damgaard and M. Molinari, Nucl. Phys. A127 (1969) 429.

9. Y. Terrien, Nucl. Phys. A215 (1973) 29.

10. H. V. Geramb, R. Sprickmann, and G. L. Strobel, Nucl. Phys. A199 (1973) 545.

11. H. V. Geramb, private communication.

12. W. T. Wagner, G. M. Crawley, G. R. Hammerstein, and H. McManus, Phys. Rev. C12 (1975) 757.

13. W. P. Alford and D. G. Burke, Phys. Rev. 185 (1969) 1560; R. A. Moyer, B. L. Cohen, and R. C. Diehl, Phys. Rev. C2 (1970) 1898; S. M. Smith et. al, Nucl. Phys. A173 (1971) 32.

14. C. Glashausser, B. G. Harvey, D. L. Hendrie, J. Mahoney, E. A. McClutchie and J. Saudinos, Phys. Rev. Letters 21 (1968) 918.

15. W. T. Wagner, G. R. Hammerstein, G. M. Crawley, J. R. Borysowicz and F. Petrovich, Phys. Rev. C8 (1973) 2504.

16. W. T. Wagner, G. M. Crawley and G. R. Hammerstein, Phys. Rev. C11 (1975) 486.

17. J. B. Ball, IEEE Trans. Nucl. Sci. NS-B(4) (1966) 340.

18. M. L. Whiten, University of Georgia dissertation, 1970 (unpublished).

19. C. B. Fulmer, J. B. Ball, A. Scott, and M. L. Whiten, Phys. Rev. 181 (1969) 1565.

20. G. Vallois, J. Saudinos, O. Beer, M. Gendrot and P. Lopato, Phys. Letters 22 (1966) 659; J. C. Hafele and R. Woods, Phys. Letters 23 (1966) 579.

21. M. R. Schmorak and R. L. Auble, Nucl. Data B5 (1971) 211.

22. M. Lewis, F. Bertrand and C. B. Fulmer, Phys. Rev. C7 (1973) 1966.

23. G. R. Hammerstein, private communication.

24. E. C. Halbert and G. R. Satchler, Nucl. Phys. A233 (1974) 265.

25. W. T. H. van Oers, Huang Haw, N. E. Davison, A. Ingemarsson, B. Fagerstrom and G. Tibell, Phys. Rev. C10 (1974) 307.

26. J. C. Hafele, Phys. Rev. 159 (1967) 996.

27. O. Hausser, F. C. Khanna and D. Ward, Nucl. Phys. A194 (1972) 113.

28. W. G. Love and G. R. Satchler, Nucl. Phys. A101 (1967) 424.

29. W. G. Love and G. R. Satchler, Nucl. Phys. A159 (1970) 1.

30. W. G. Love and L. J. Parish, Nucl. Phys. A157 (1970) 625.

31. J. Raynal, Trieste Lectures (1971); W. G. Love, Phys. Letters 35B (1971) 371.

32. F. Petrovich, Nucl. Phys. A203 (1973) 65 and references cited therein.

33. G. R. Satchler, Phys. Letters 35B (1971) 279.

34. W. G. Love and L. W. Owen, Nucl. Phys. A239 (1975) 74.

FIGURE CAPTIONS

Figure 1 Collective model fit to the experimental data for the excitation of the doublet at E_{ex}=2.61 MeV by 61.2 MeV protons.

Figure 2 Comparison between the collective model calculation and the experimental cross sections for the excitation of the first four excited states in ^{207}Pb by 61.2 MeV protons.

Figure 3 Comparison of the experimental cross sections for populating the first four excited states at E_p=61.2 MeV with those predicted by the microscopic model (including macroscopic core polarization). The valence, core and imaginary contributions are denoted by V, C and I respectively. The core contribution includes the imaginary part; the valence term does not.

Figure 4 Comparison of the experimental cross sections for populating the first four excited states at E_p=20.2 MeV with those predicted by the collective (---) and microscopic (————) models. V, C and I are as defined for fig. 3.

TABLE 1

Differential Cross Sections for States in ^{207}Pb Excited by 61.2 MeV Protons

$\theta_{c.m.}$ (deg.)	$\frac{5}{2}^-$ (0.570 MeV)	$\frac{3}{2}^-$ (0.898 MeV)	$\frac{11}{2}^+$ (1.63 MeV)	$\frac{7}{2}^-$ (2.34 MeV)	$\frac{5}{2}^+,\frac{7}{2}^+$ (2.64 MeV)
13.06					$1.40\pm0.03\times10^{1}$
14.07					1.38 ± 0.03
15.08	$6.30\pm0.80\times10^{-1}$	$5.50\pm0.52\times10^{-1}$			1.28 ± 0.04
16.08	6.27 ± 0.59	4.16 ± 0.72		$2.89\pm0.51\times10^{-1}$	1.25 ± 0.06
17.08		3.51 ± 0.52			1.11 ± 0.05
18.09		3.93 ± 0.55		3.65 ± 0.40	1.24 ± 0.03
20.10		1.52 ± 0.25	$9.84\pm2.42\times10^{-2}$	2.93 ± 0.30	1.07 ± 0.05
20.60				2.90 ± 0.40	
22.11				2.68 ± 0.34	$7.96\pm0.36\times10^{0}$
24.12				2.35 ± 0.25	5.36 ± 0.27
26.12	3.09 ± 0.34			2.23 ± 0.22	3.95 ± 0.16
27.62	2.82 ± 0.21		$1.30\pm0.17\times10^{-1}$	1.69 ± 0.17	3.39 ± 0.16
28.13	2.53 ± 0.22		1.09 ± 0.14	1.35 ± 0.14	3.36 ± 0.16
29.14	2.29 ± 0.18		1.03 ± 0.10	1.21 ± 0.10	3.69 ± 0.16
30.14	1.94 ± 0.13		$9.38\pm0.87\times10^{-2}$	1.07 ± 0.08	3.64 ± 0.15
32.15				$9.89\pm0.74\times10^{-2}$	4.38 ± 0.18
33.15	$9.18\pm1.20\times10^{-2}$	$6.19\pm0.90\times10^{-2}$			
34.16				$1.09\pm0.08\times10^{-1}$	
35.17	7.27 ± 0.90	5.45 ± 0.91			
36.17				1.17 ± 0.07	3.23 ± 0.14
38.18	7.63 ± 0.98			1.15 ± 0.08	2.29 ± 0.10
41.19	8.15 ± 0.79	5.38 ± 0.77			1.27 ± 0.06
43.19	$1.03\pm0.10\times10^{-1}$	8.40 ± 1.01			
44.20	1.10 ± 0.07		4.39 ± 0.39	$7.00\pm0.42\times10^{-2}$	
46.21		4.23 ± 0.71			
47.21	$8.35\pm0.94\times10^{-2}$	3.41 ± 0.65	2.16 ± 0.30		1.57 ± 0.03
49.22	5.16 ± 0.57		2.68 ± 0.50		1.71 ± 0.08
51.22	3.25 ± 0.49			3.53 ± 0.41	
52.22	2.45 ± 0.54		2.63 ± 0.50	3.64 ± 0.54	1.07 ± 0.05
54.23	3.60 ± 0.43		2.03 ± 0.37	4.09 ± 0.40	$8.88\pm0.39\times10^{-1}$
55.23	3.31 ± 0.47	3.06 ± 0.43			
57.24	3.43 ± 0.47	3.03 ± 0.40			4.28 ± 0.22
58.24	4.20 ± 0.44	4.53 ± 0.47	2.47 ± 0.29	3.80 ± 0.36	4.76 ± 0.21
60.25	3.49 ± 0.26	3.49 ± 0.30	2.15 ± 0.38	2.47 ± 0.30	5.28 ± 0.24
62.25	2.08 ± 0.24	2.26 ± 0.29	1.06 ± 0.24	1.54 ± 0.24	6.06 ± 0.26
65.26	1.60 ± 0.34	1.20 ± 0.27		$9.5\pm2.2\times10^{-3}$	6.88 ± 0.31
68.26			$7.8\pm1.5\times10^{-3}$	$1.35\pm0.19\times10^{-2}$	4.16 ± 0.20
70.27	$9.4\pm2.5\times10^{-3}$	$6.5\pm1.6\times10^{-3}$	4.8 ± 1.5	$8.4\pm1.9\times10^{-3}$	2.97 ± 0.15
73.27	8.6 ± 1.8	5.8 ± 1.1	4.9 ± 1.6	8.1 ± 1.6	2.01 ± 0.10
76.28	6.0 ± 1.4	4.0 ± 1.4	5.2 ± 1.7	6.1 ± 1.8	2.19 ± 0.11
80.28	4.4 ± 1.3	1.5 ± 0.8	1.7 ± 0.7	5.0 ± 1.5	2.22 ± 0.12
85.28	4.5 ± 1.4	2.8 ± 0.9	3.1 ± 0.9	3.5 ± 1.0	1.47 ± 0.08
90.28	5.3 ± 1.5			1.6 ± 0.6	$8.0\pm0.6\times10^{-2}$
95.28			1.7 ± 1.0		6.5 ± 0.50
100.28	2.3 ± 0.9	1.2 ± 0.6			6.4 ± 0.50
105.28					3.1 ± 0.26

Expressed in mb/sr in c.m.s. Errors quoted include counting statistics, an estimate of uncertainties in the background subtraction and an estimate of the reproducibility of the track counting.

TABLE 2

Comparison of deformation parameters obtained with different optical models

Nucleus	E_{ex} (MeV)	L	E_p (MeV)	BFOM[a] β_L	BFOM[a] $\beta_E - \beta_{61}$ %	HSOM[b] β_L	HSOM[b] $\beta_E - \beta_{61}$ %	$\beta_{HS} - \beta_{BF}$ %	BGOM[c] β_L	BGOM[c] $\beta_{BG} - \beta_{BF}$ %
			20.2	0.029	+7.4	0.031	+10.7	+2.2		
^{207}Pb	0.570	2	35.0	0.033	+22.2	0.035	+25.0	+6.1	0.034	+3.0
			61.2	0.027		0.028		+3.7		
			EM[d]	0.027[d]	0.0	0.027[d]	+3.5			
			20.2	0.036	+24.1	0.035	+16.7	-2.7		
^{207}Pb	0.898	2	35.0	0.033	+13.8	0.036	+20.0	+9.1	0.040	+21.2
			61.2	0.029		0.030		+3.4		
			EM[d]	0.025[d]	-13.8	0.025[d]	-16.7			
			20.2	0.046	+58.6	0.049	+58.1	+6.5		
^{207}Pb	2.34	4	35.0	0.033	+13.8	0.039	+18.2	+18.2	0.036	+9.1
			61.2	0.029		0.031		+6.9		
			20.2	0.036	+56.5	0.040	+51.9	+11.1		
^{207}Pb	1.63	7	35.0	0.029	+26.1	0.031	+14.8	+6.9	0.028	-3.4
			61.2	0.023		0.027		+17.4		
			35.0						0.116[e]	
^{207}Pb	2.64 Doublet	3	61.2	0.103		0.100				
			61.2	0.100[f]						
^{208}Pb	2.614	3	61.2	0.103[g]		0.098[g]				
^{209}Bi	2.62 Multiplet	3	61.2	0.101[g]		0.095[g]				
			61.2	0.098[f]						

[a] 'Best fit' optical model parameters from references 14, 23, and 19 respectively.
[b] Halbert and Satchler energy dependent parameters for ^{208}Pb, reference 24.
[c] Bechetti and Greenlees optical model, reference 23.
[d] Electromagnetic values, reference 27.
[e] Sum of β_3^2 from reference 16.
[f] Measured cross sections ~f. measured ^{208}Pb cross section, assumes $\beta_{208} = 0.103$
[g] Corrected values, earlie. values were incorrect.

TABLE 3

Microscopic model core-coupling parameters and effective charges, collective deformation parameters

E_{ex} MeV	J_i^π	J_f^π	L	E_p MeV	Λ_L^a		e_{eff}	
0.570	$\frac{1}{2}^-$	$\frac{5}{2}^-$	2	20.2	0.033	(0.031)[b]	1.0	(1.0)[b]
				35.0	0.030[c]		0.95	(0.85)[d]
				61.2	0.020	(0.025)[b]	0.63	(0.79)[b]
				EM	0.030[e]		0.95	
0.898	$\frac{1}{2}^-$	$\frac{3}{2}^-$	2	20.2	0.030	(0.030)[b]	0.83	(0.83)[b]
				35.0	0.027[c]		0.74	(0.87)[d]
				61.2	0.020	(0.027)[b]	0.55	(0.74)[b]
				EM	0.028[e]		0.76	
2.34	$\frac{1}{2}^-$	$\frac{7}{2}^-$	4	20.2	0.038	(0.038)[b]	0.99	(0.99)[b]
				35.0	0.023[c]		0.61	(0.78)[d]
				61.2	0.015	(0.019)[b]	0.39	(0.49)[b]
1.63	$\frac{1}{2}^-$	$\frac{13}{2}^+$	7	20.2	0.030	(0.030)[b]	0.69	(0.69)[b]
				35.0	0.019[c]		0.43	(0.41)[d]
				61.2	0.010	(0.012)[b]	0.23	(0.28)[b]

[a] 'Best fit' optical model parameters except where stated otherwise, collective core polarization

[b] Central interaction normalized by elastic volume integrals from experiments

[c] Reference 15

[d] 'Microscopic core' calculations, reference 15

[e] Reference 27

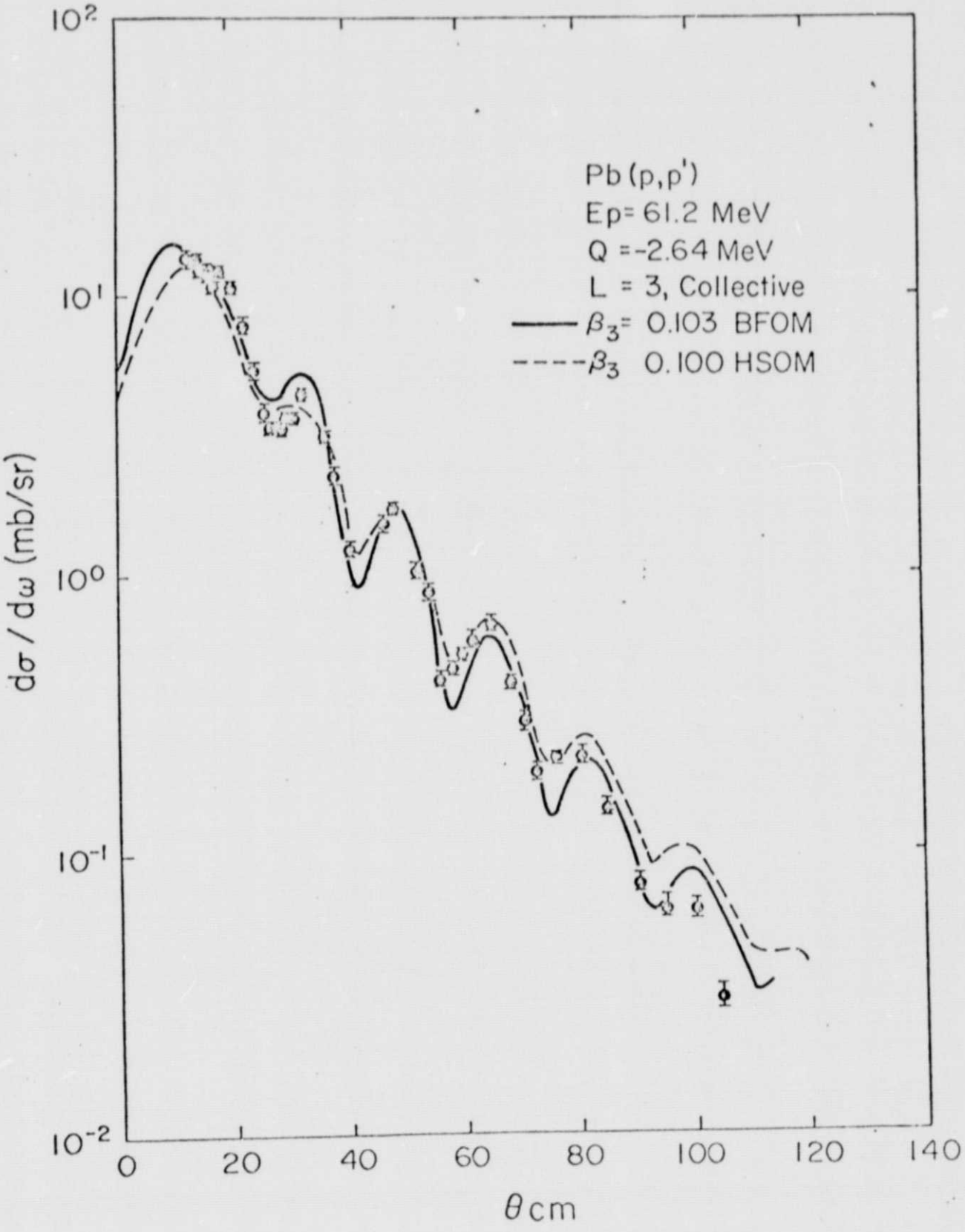
Pb (p,p')
Ep= 61.2 MeV
Q =-2.64 MeV
L = 3, Collective
β_3= 0.103 BFOM
β_3 0.100 HSOM
10^2
10^1
10^0
10^{-1}
10^{-2}
dσ / dω (mb/sr)
0
20
40
60
80
100
120
140
θcm

Fig. 1.

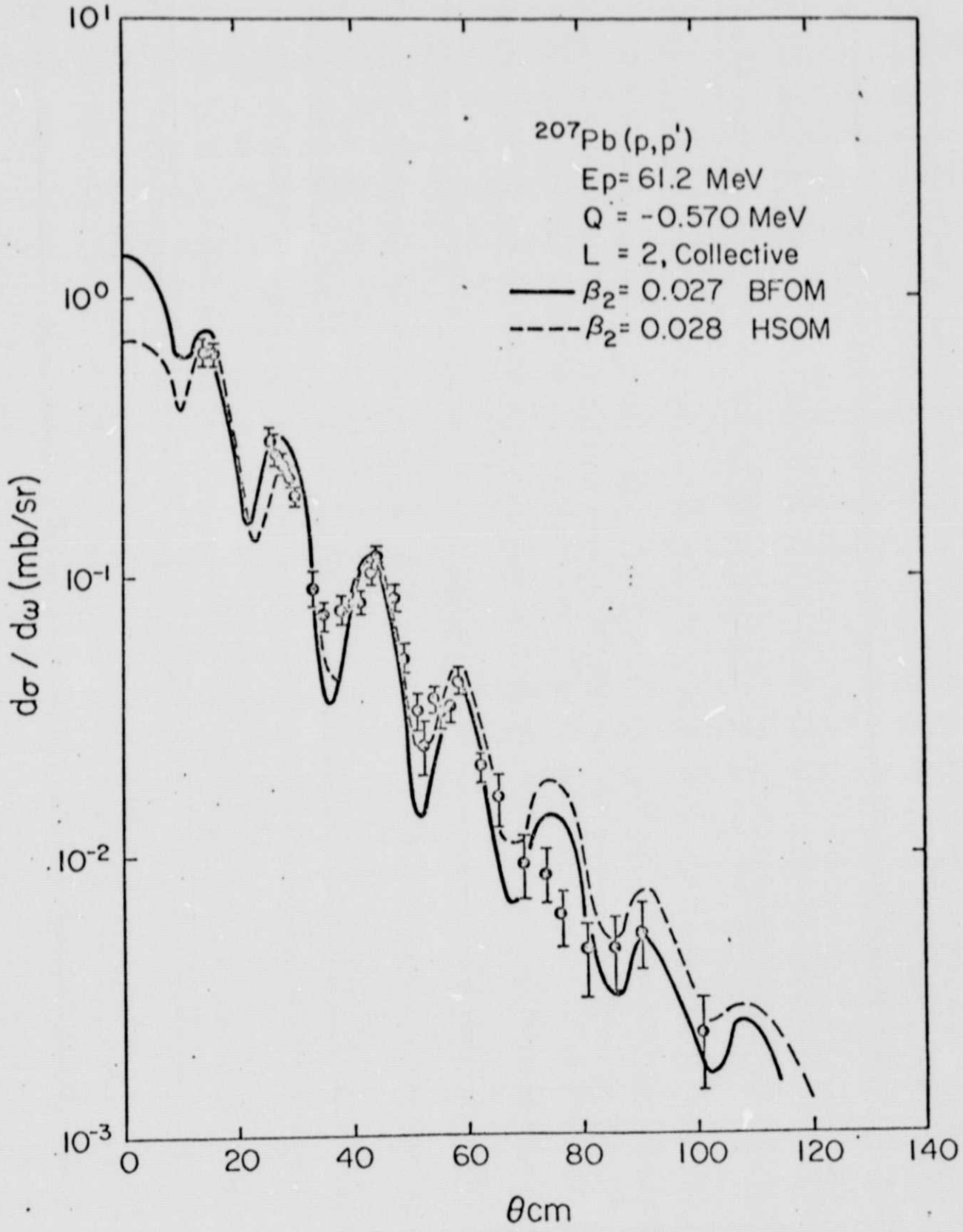
^{207}Pb (p,p')
Ep= 61.2 MeV
Q = -0.570 MeV
L = 2, Collective
β_2= 0.027 BFOM
β_2= 0.028 HSOM
dσ / dω (mb/sr)
θcm
10¹
10⁰
10⁻¹
10⁻²
10⁻³
0
20
40
60
80
100
120
140

Fig. 2(a)

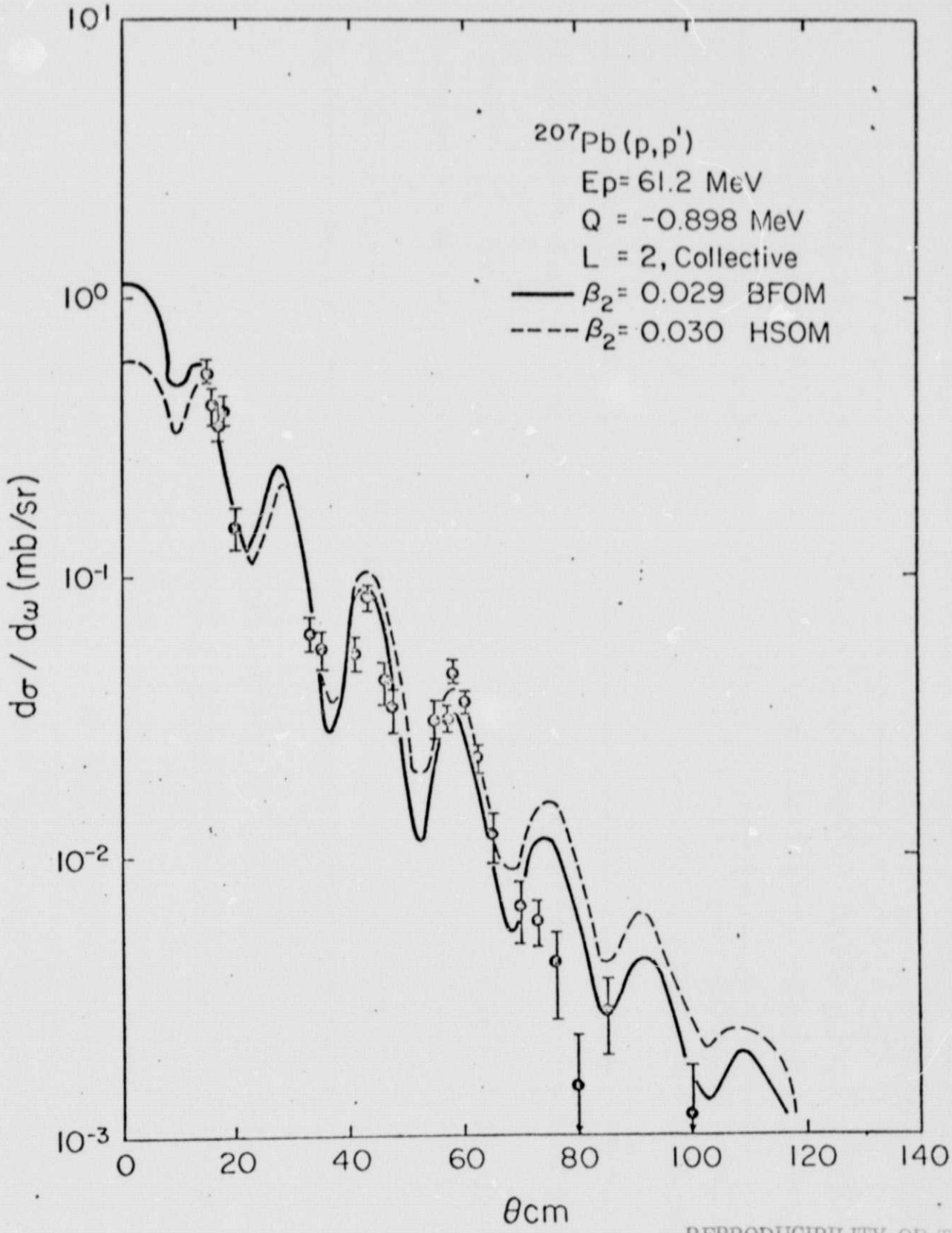

Fig. 2(b)

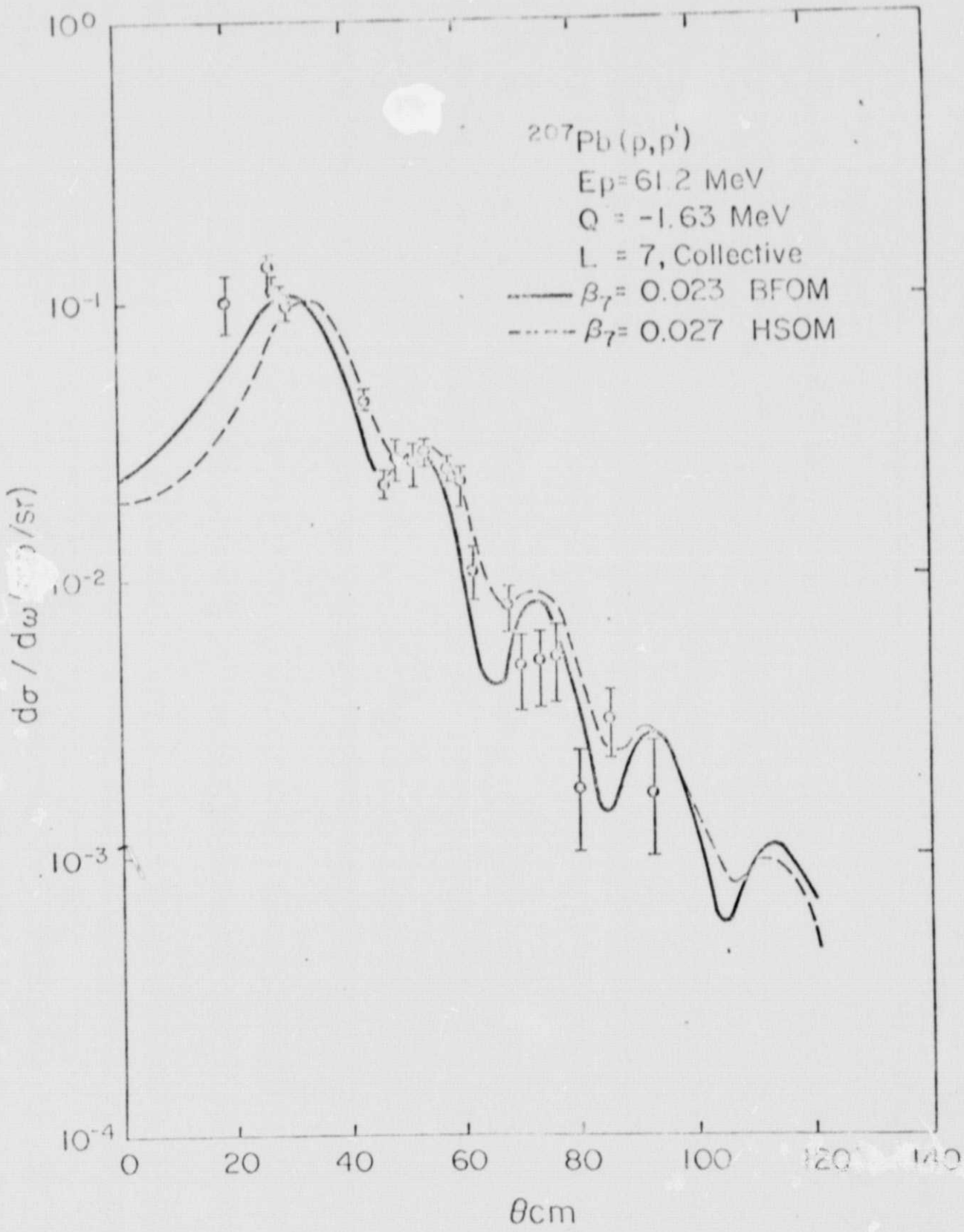
^{207}Pb(p,p')
Ep= 61.2 MeV
Q = -1.63 MeV
L = 7, Collective
β_7= 0.023 BFOM
β_7= 0.027 HSOM
dσ / dω' (mb/sr)
θcm
10^0
10^-1
10^-2
10^-3
10^-4
0
20
40
60
80
100
120
140

Fig. 2(c)

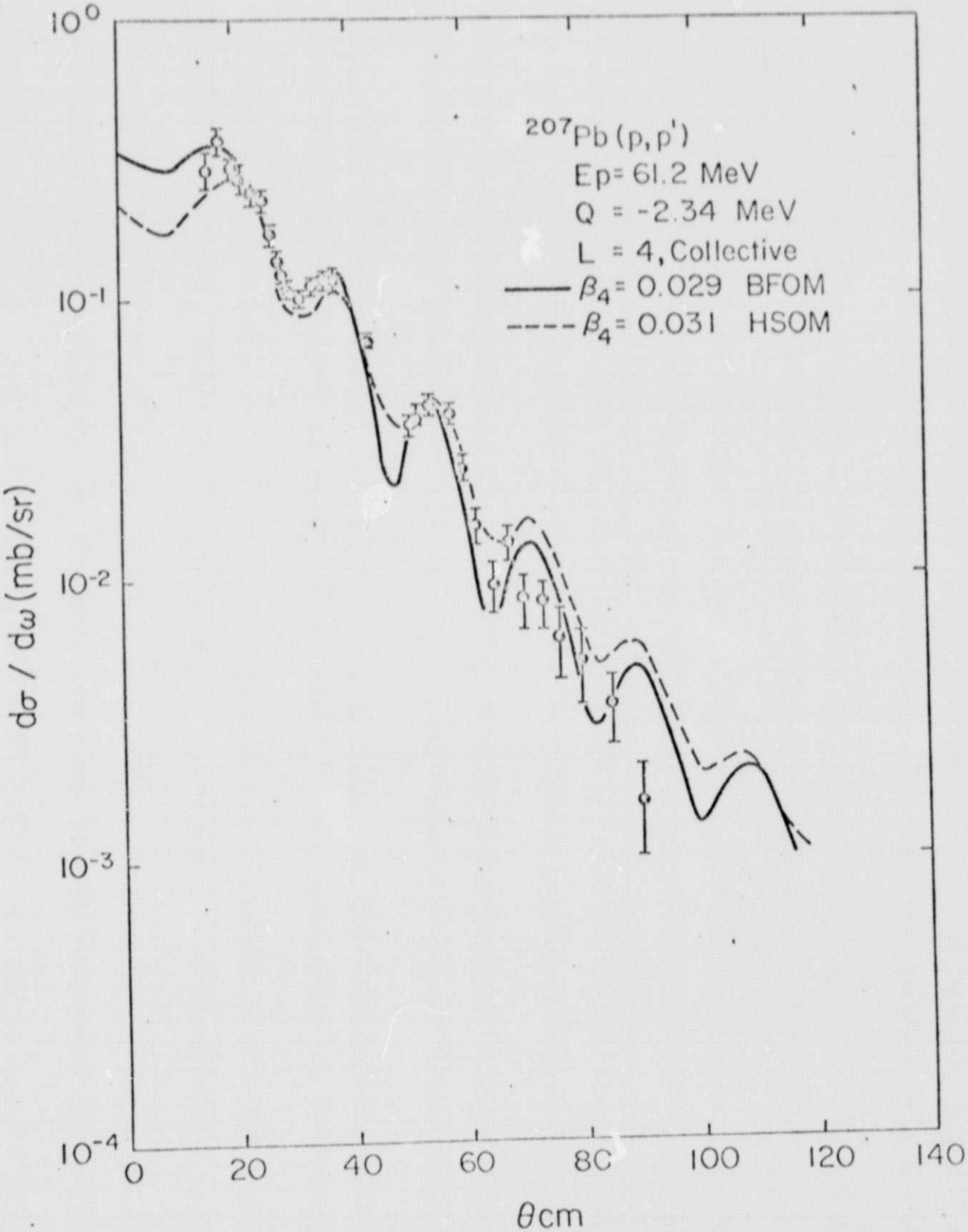
^{207}Pb (p, p')
Ep = 61.2 MeV
Q = -2.34 MeV
L = 4, Collective
β_4 = 0.029 BFOM
β_4 = 0.031 HSOM
dσ / dω (mb/sr)
θcm
10^0
10^-1
10^-2
10^-3
10^-4
0
20
40
60
80
100
120
140

Fig. 2(d)

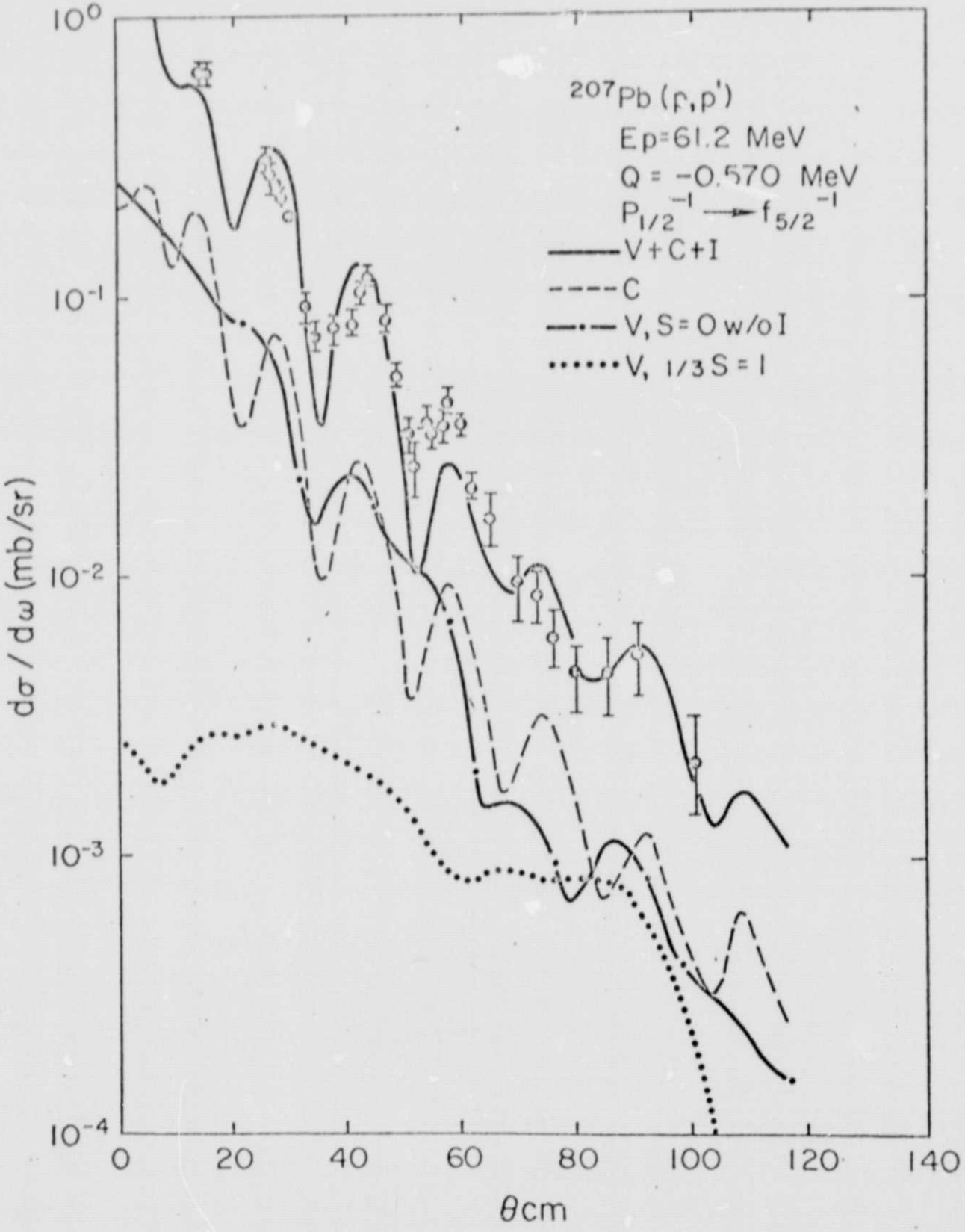
^{207}Pb (p,p')
Ep=61.2 MeV
Q = −0.570 MeV
$P_{1/2}^{-1} \rightarrow f_{5/2}^{-1}$
V+C+I
C
V, S=0 w/o I
V, 1/3 S=1
dσ / dω (mb/sr)
θcm
10^0
10^{-1}
10^{-2}
10^{-3}
10^{-4}
0
20
40
60
80
100
120
140

Fig. 3(a)

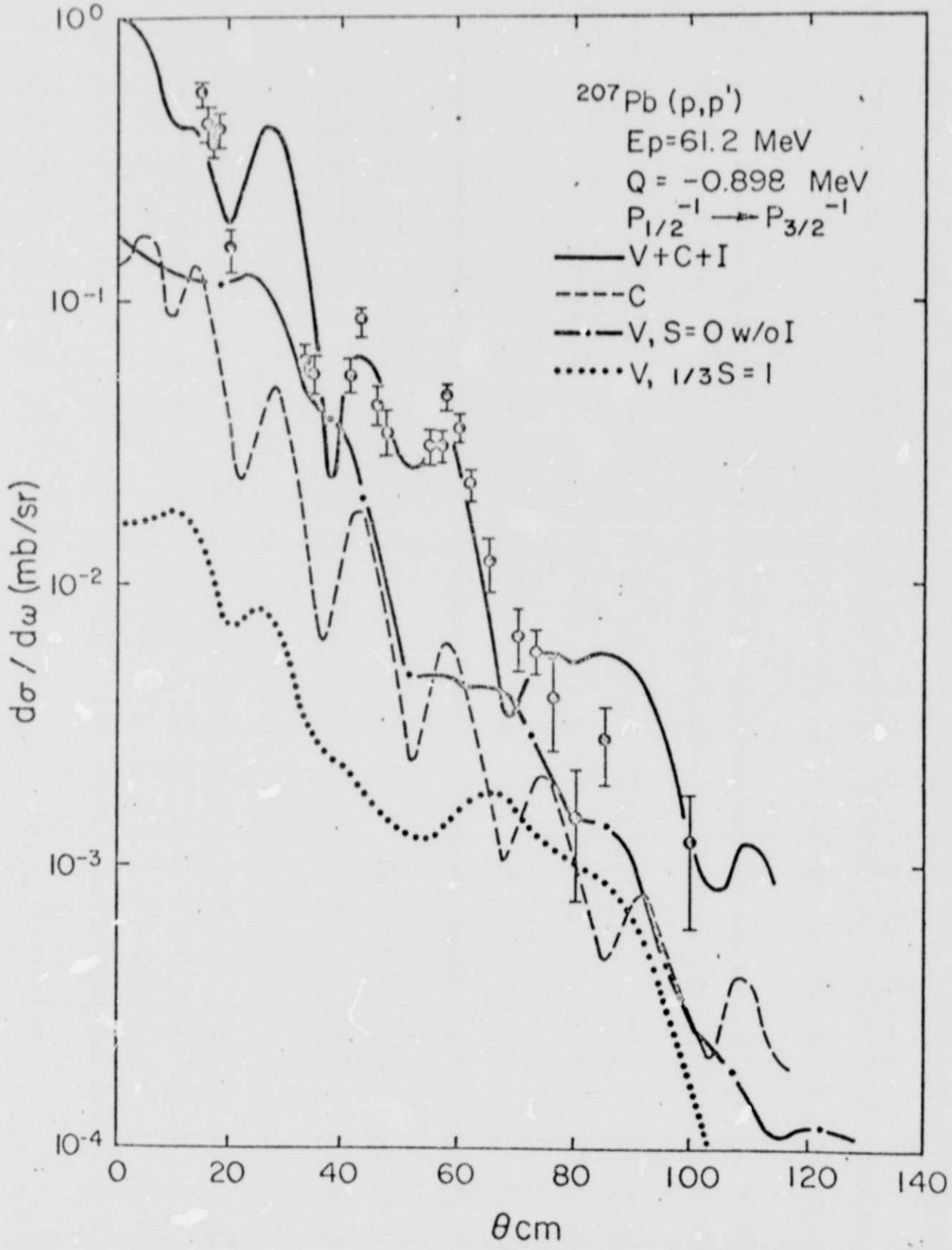

Fig. 3(b)

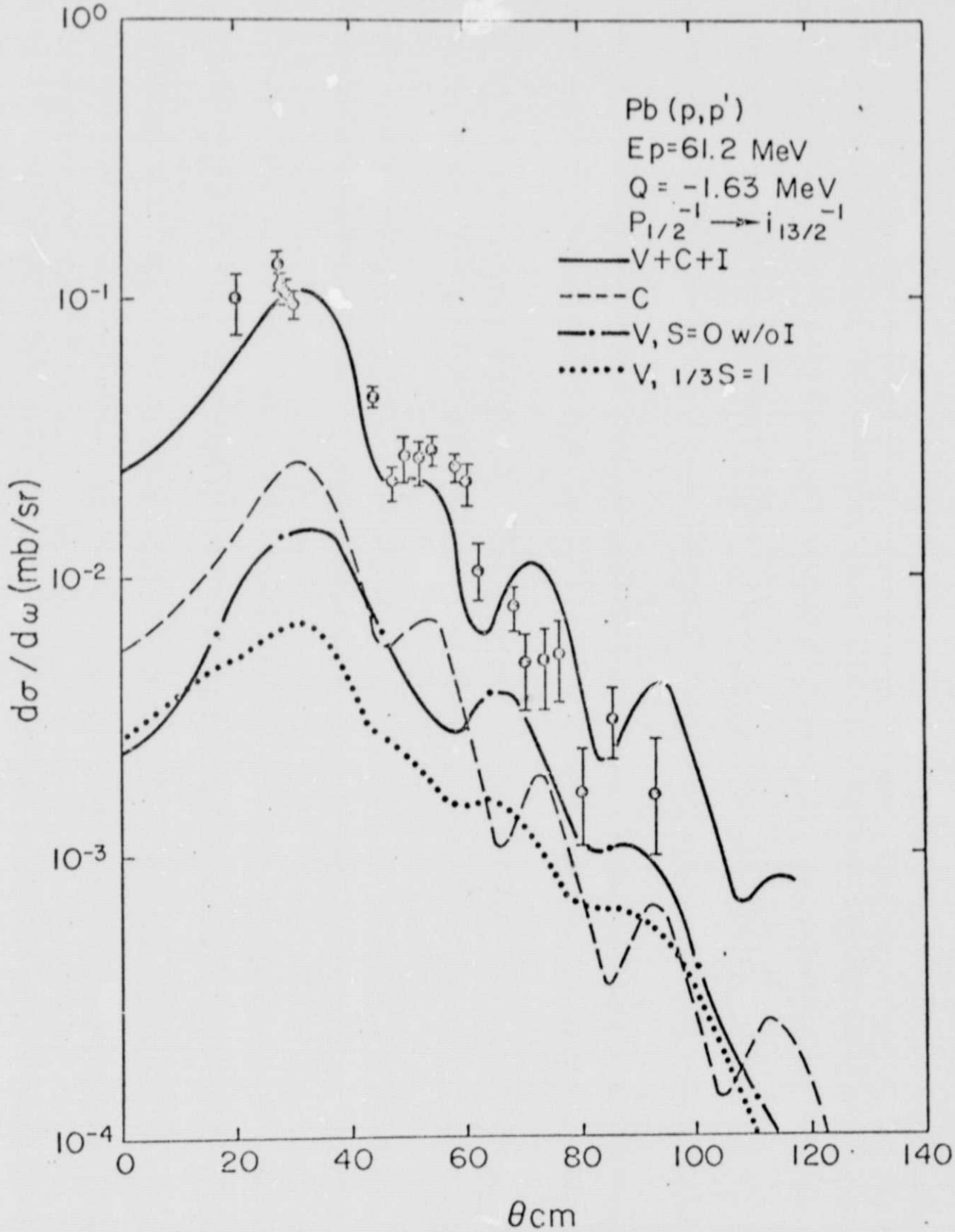
Pb (p,p')
Ep=61.2 MeV
Q = -1.63 MeV
$P_{1/2}^{-1} \rightarrow i_{13/2}^{-1}$
V+C+I
C
V, S=0 w/oI
V, 1/3S=1
10^0
10^{-1}
10^{-2}
10^{-3}
10^{-4}
$d\sigma / d\omega$ (mb/sr)
0
20
40
60
80
100
120
140
θcm

Fig. 3(c)

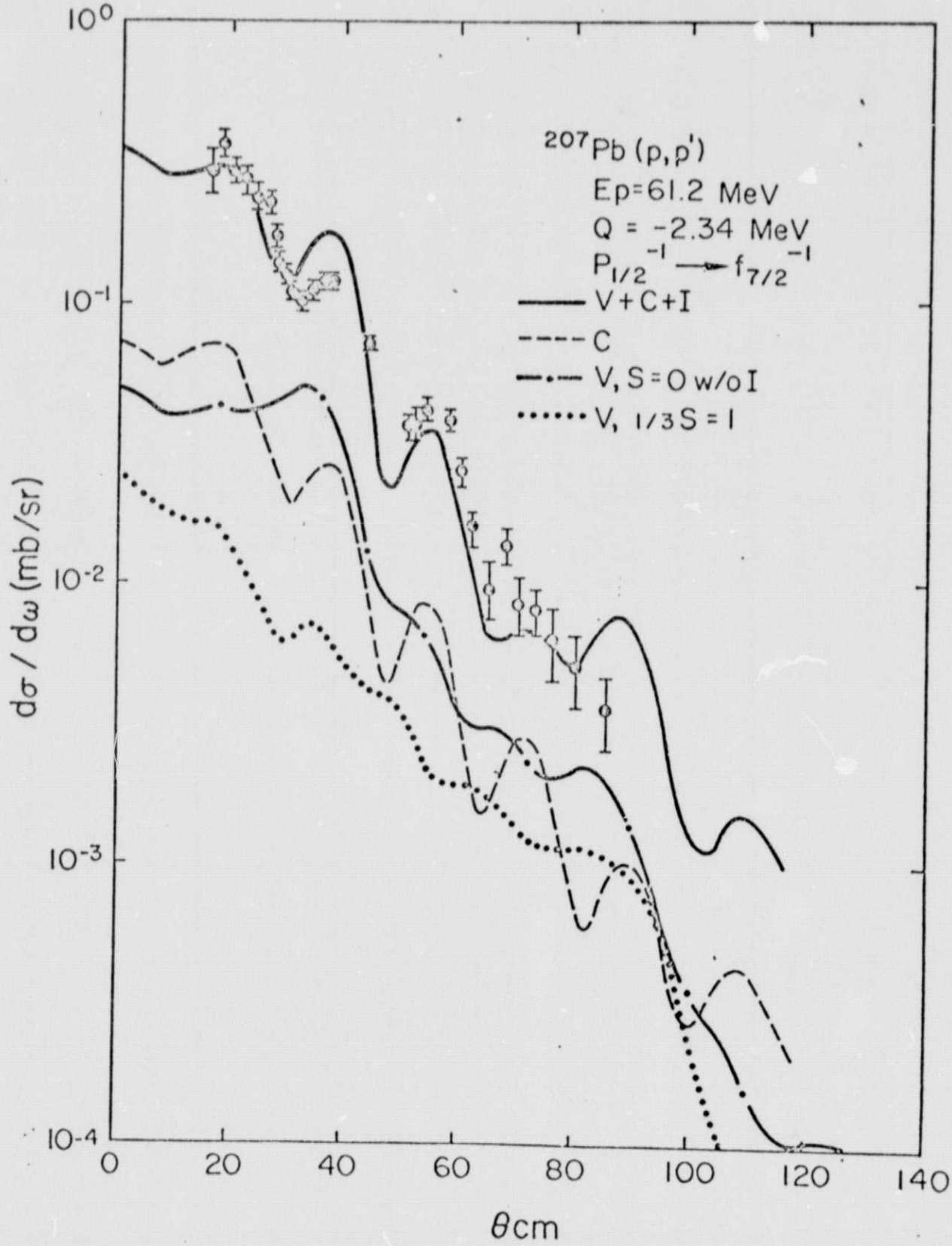
^{207}Pb (p,p')
Ep=61.2 MeV
Q = -2.34 MeV
$P_{1/2}^{-1} \rightarrow f_{7/2}^{-1}$
V+C+I
C
V, S=0 w/o I
V, 1/3 S = I
dσ / dω (mb/sr)
θcm
10^0
10^-1
10^-2
10^-3
10-4
0
20
40
60
80
100
120
140

Fig. 3(d)

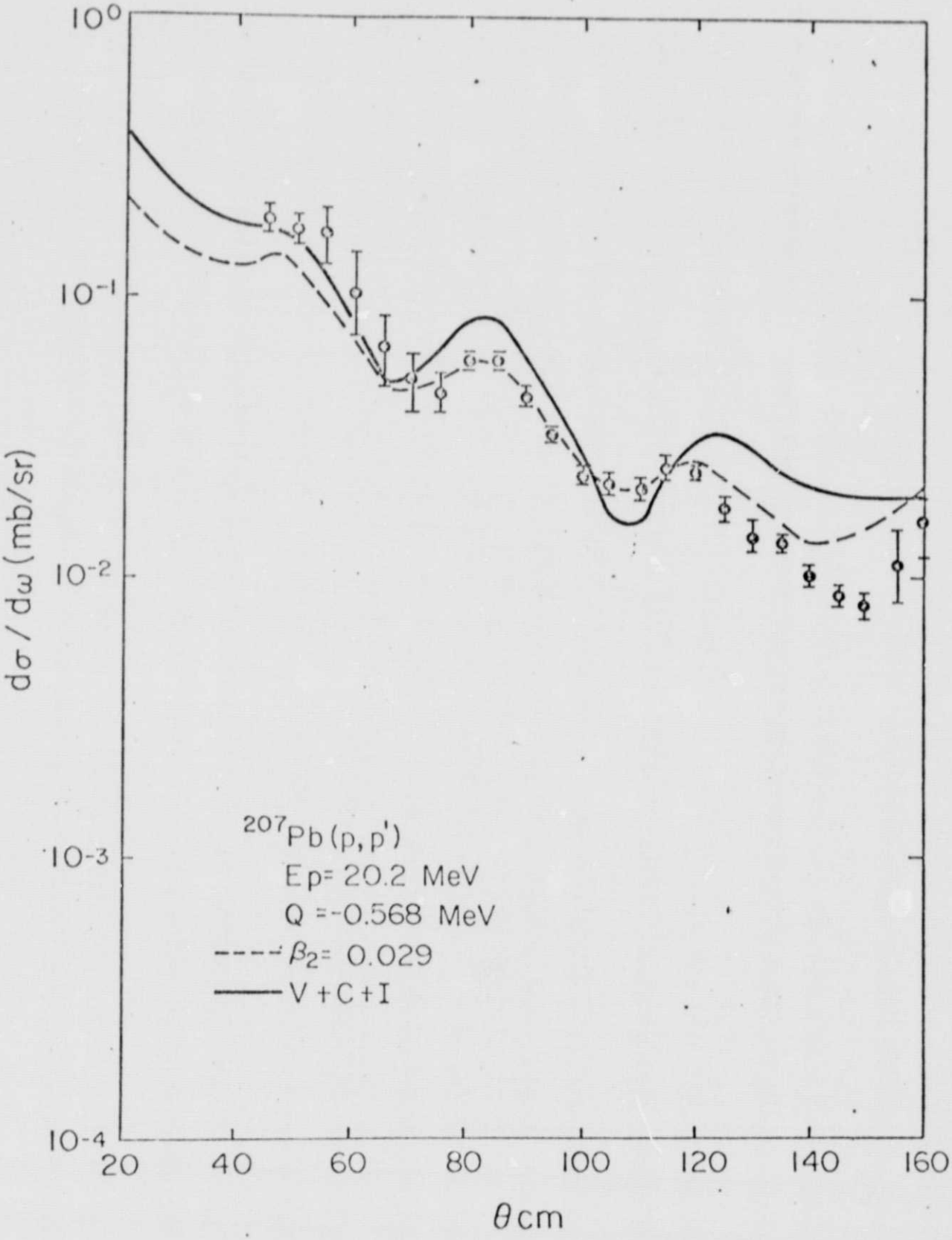
10^0
10^-1
10^-2
10-3
10-4
dσ / dω (mb/sr)
20
40
60
80
100
120
140
160
θcm
207Pb (p, p')
Ep= 20.2 MeV
Q =-0.568 MeV
β2= 0.029
V + C + I

Fig. 4(a)

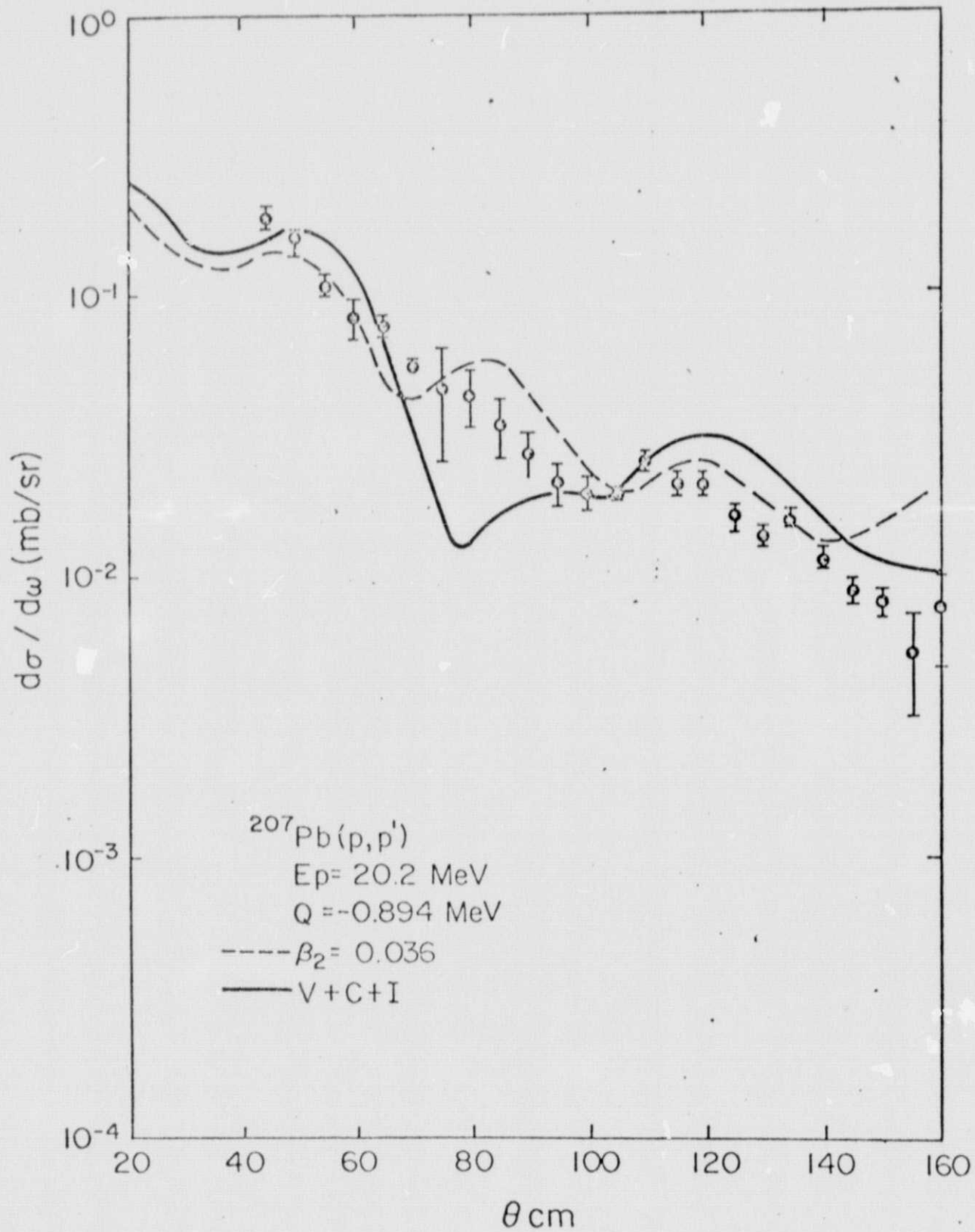
10^0
10^-1
10^-2
10^-3
10^-4
dσ / dω (mb/sr)
20
40
60
80
100
120
140
160
θ cm
207Pb(p,p')
Ep= 20.2 MeV
Q =-0.894 MeV
----β2= 0.036
——V+C+I

Fig. 4(b)

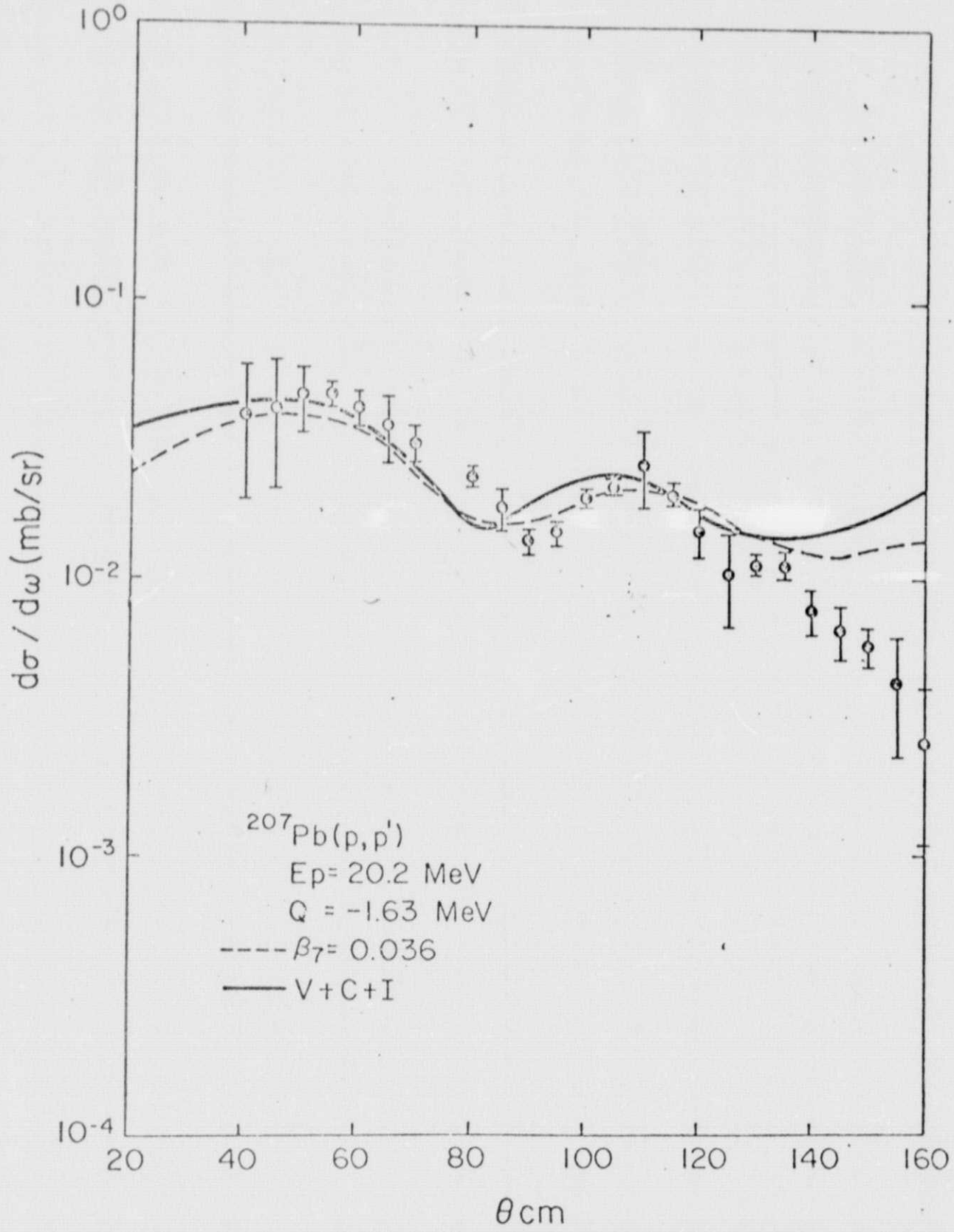
10^0
10^{-1}
10^{-2}
10^{-3}
10^{-4}
$d\sigma / d\omega$ (mb/sr)
^{207}Pb(p,p')
Ep= 20.2 MeV
Q = -1.63 MeV
---- β_7= 0.036
—— V+C+I
20
40
60
80
100
120
140
160
θcm

Fig. 4(c)

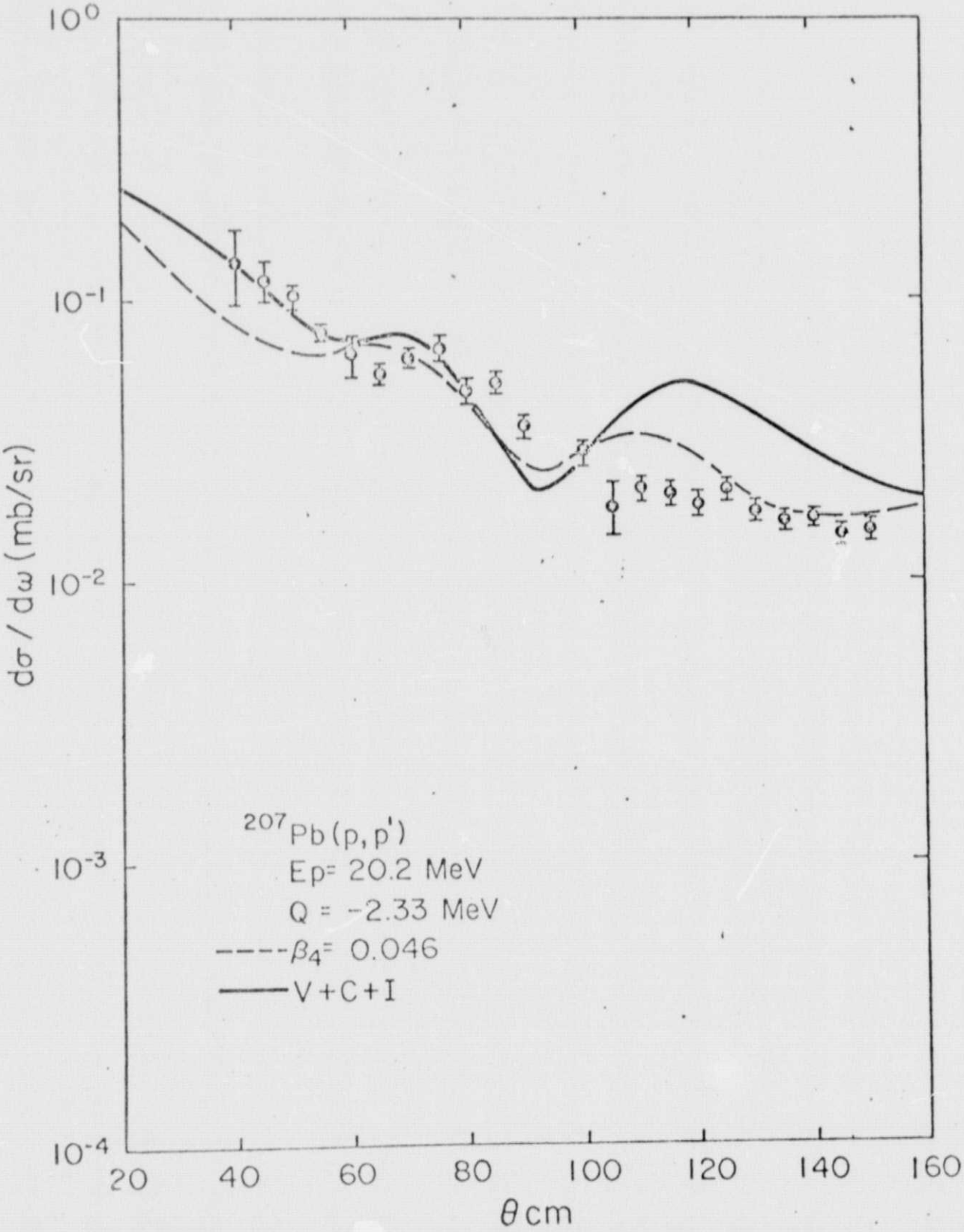
10^0
10^-1
10^-2
10^-3
10^-4
dσ / dω (mb/sr)
20
40
60
80
100
120
140
160
θcm
207Pb(p,p')
Ep= 20.2 MeV
Q = -2.33 MeV
----β4= 0.046
——V+C+I

Fig. 4(d)